AA10 - Predictive Analysis of Industrial Precipitation Cycles Using Population Balance and Deep Learning Methods

Vladimir Golubev[1], Dmitriy Chistyakov[2] and Iliya Blednykh[3]
1. Head of Department
2. Chief Engineer
3. Data Science Specialist
RUSAL ETC, Saint Petersburg, Russia
Corresponding author: Vladimir.Golubev2@rusal.com

Abstract

Existing advanced control systems are not very accurate in the prediction of the aluminum hydroxide particle size distribution (PSD) and liquor productivity in the precipitation circuits of alumina refineries. The main reasons for this are low rates and high noise contamination of the controlled processes, and big differences in time constants for various parameters. This paper discusses some alternatives for prediction of the precipitation process, i.e. population balance method (PBM) and deep learning method. Though different in their characteristics and possibilities, these methods complement each other. This study also shows that updated PBM equations can be used to predict the main trend and inflection points of PSD oscillation curves, and calculate A/C ratio of the spent liquor over the extended periods. Besides, the set of LSTM blocks enables the creation of artificial neural networks for short-term periods. The predictive capability of such networks is sufficient to perform optimum control of industrial precipitation processes. To operate both methods a specialized software PrecipExpert was developed. The software is designed to develop, configure and fine-tune a consolidated data system of the precipitation area. The developed automated system is currently being tested at the RUSAL Kamensk-Uralsky Alumina Refinery (Russia).

Keywords: Advanced process control, precipitation, population balance, deep learning, self-oscillations.

1. Problems of Precipitation Control at the Refinery

Advanced Process Control (APC) is a method for the optimal control of multivariable objects based on a specified criterion. Such systems comprise a model of the controlled object used to predict the response of the object to the controlled variable(s), and an optimization algorithm that solves the problem with a global extremum (or maximum) for a given criterion under given constraints.

This type of control system has been used in alumina refineries for a long time, to control for example, the parameters of digestion trains, washing lines, and calciners. In the precipitation area they are used to solve secondary problems, such as stream distribution between parallel lines of precipitators, stabilization of the slurry solids content and controlling the temperature in precipitator tanks. Stabilizing the PSD of aluminum hydroxide and increasing liquor productivity are far more challenging tasks for automated control, and such tasks are still managed by process engineers. The theory of automation control attributes the limited use of APC for PSD and liquor productivity control to the specifics of the process (see Table 1).

These process specifics cause control instability; the optimum is not found, self-oscillations appear, and an inverse response of the object to the applied action is observed.

Table 1. Process specifics causing difficulty with PSD and liquor productivity control in the precipitation area.

Process specifics	Examples
Many noisy signals with low Signal-to-Noise ratio	Noise can be caused by changing concentration of solids, injection of fine particles after chemical cleaning of precipitators, varying liquor impurities, daily temperature fluctuations and equipment breakdowns
Low Time-to-Steady-State values	The rate of nucleation and the rate of particle removal from the system are low with respect to the total number of crystals
Inability to directly measure key parameters	The quality of the crystal surface, the number of true nuclei, interface area cannot be measured directly
Big difference in time constants for parameters	Flow is measured at intervals of minutes; A/C and temperature are measured in intervals of hours; PSD is measured in intervals of days or weeks
Presence of the parameters with a strong functional relation	Liquor yield and PSD are functionally related; crystal coarsening causes a decrease in yield and vice versa, making their simultaneous control challenging

Presently the main method for simulating seeded crystallization is the population balance method (PBM). The method is based on sufficiently strict physical and chemical laws to provide for the complete understanding of the ongoing processes. Unfortunately, the literature does not report any examples of the successful use of PBM in actual production control, although this method is widely used in laboratory tests. Population balance models are difficult to set up, and their use for process control would require significant computational resources.

Recently, interest has been focused on predictions by machine learning methods (ML), more specifically, artificial neural networks (ANN). This type of model has become widely used due to its high general performance, the ability to use available historical data to train ANN, and high predictive performance. Among its disadvantages are: the inability to explain why ANN generates this or that forecast, and the loss of the prediction quality of over time due to the shift in the characteristics of the controlled object.

This study aimed to develop mathematical models of both types (population balance equation and machine learning method), for an existing industrial facility – the precipitation area at the RUSAL Kamensk Uralsky alumina refinery (UAZ). Based on the simulation results, the forecasts of each of the models can be compared, allowing the assessment of their applicability.

2. Particle Population Balance Method

An analytical method for the simulation of mass crystallization is well developed. It is based on the compilation and solution of a system of population balance equations.

The generalized population balance equation relates the number of particles in PSD grades to the rate of linear crystal growth, agglomeration, nucleation and breakage of particles [1]:

$$\frac{\partial n_i}{\partial t} + G\frac{\partial n_i}{\partial u} = B_i - D_i \quad (1)$$

where:

n_i number of particles in the ith grade

t time, s

G	rate of linear growth, m/s
u	particle grade coordinate in PSD
B_i and D_i	rate of particles birth and death in the ith grade respectively, 1/(m^4·s).

The rate of linear growth corresponds to the following dependency [2]:

$$\mathrm{G} = \mathrm{k_0}\exp\left(\frac{\mathrm{E_{act}}}{\mathrm{RT}}\right)\left(\frac{\mathrm{A}-\mathrm{A_{eq}}}{\mathrm{C}}\right)^{\mathrm{z1}} \tag{2}$$

where:

k_0	pre-exponential factor of the linear growth rate constant
E_{act}	activation energy, J/mol
T	temperature, K
A_{eq}	equilibrium concentration of alumina in the liquor, g/L
$z1$	supersaturation exponent
C	concentration of caustic alkali expressed as Na_2CO_3, g/L.

The agglomeration model was proposed by Livk and Ilievski [3,4]. The agglomeration rate is calculated for each grade of particles by the following formula:

$$\left.\frac{\partial \mathrm{n_i}}{\partial \mathrm{t}}\right|_{\mathrm{agg}} = \frac{1}{2}\int_0^{\mathrm{v}} \beta(\mathrm{v}-\mathrm{u},\mathrm{u})\cdot \mathrm{n}(\mathrm{v}-\mathrm{u})\cdot \mathrm{n}(\mathrm{u})\mathrm{du} - \mathrm{n}(\mathrm{v})\int_0^{\mathrm{N}} \beta(\mathrm{v},\mathrm{u})\cdot \mathrm{n}(\mathrm{u})\mathrm{du} \tag{3}$$

$$\beta(\mathrm{v},\mathrm{u}) = \mathrm{k_c}\frac{\mathrm{G}}{\beta_4\left(\mathrm{L_v^{1/3}}+\mathrm{L_u^{1/3}}\right)} \tag{4}$$

where:

v and u	particle grade coordinates in PSD
n	number of particles per a unit of volume
$\beta(\mathrm{v},\mathrm{u})$	function expressing the probability of particle size v and u to agglomerate
k_c	proportionality factor
β_4	correction for the agitation conditions in the tank.

The formula proposed by Misra is often used as a model for secondary nucleation [5]:

$$\mathrm{B_0} = \mathrm{k_n}\left(\frac{\mathrm{A}-\mathrm{A_{eq}}}{\mathrm{C}}\right)^{\mathrm{z2}} \mathrm{S_{sl}} \tag{5}$$

where:

B_0	nucleation rate at the left boundary of the PSD interval, 1/(m^3·s)
k_n	configurable constant of the nucleation rate, 1/(m^2·s)
S_{sl}	interface area per a unit of slurry, 1/m
$z2$	supersaturation exponent.

The breakage function is similar to the agglomeration model; for each grade of particles it is as follows:

$$\left.\frac{\partial \mathrm{n_i}}{\partial \mathrm{t}}\right|_{\mathrm{b.br}} = \left(\frac{\mathrm{L_{i+1}}}{\mathrm{L_i}}\right)^3 \vartheta_{\mathrm{i+1}}\mathrm{n_{i+1}} - \vartheta_{\mathrm{i}}\mathrm{n_i} \tag{6}$$

$$\vartheta(t,u) = k_b\gamma^p\bar{m}_1\cdot F(u). \tag{7}$$

where:

$\vartheta(t,u)$	probability function for particle breakage in the uth grade

k_b and p configurable constants
γ shear rate, 1/s
$\bar{m}_1$ normalized first moment of the crystal population per a unit of volume, 1/m^2.

The difference between the industrial process and laboratory conditions lies in the impact of many perturbing factors and a greater measurement error. Another of the serious obstacles to the application of the classical PBM model is its poor reproduction of the cyclical nature of changes in the PSD and precipitation yield. Such oscillations appear after the closure of the seed cycle (see Figure 1).

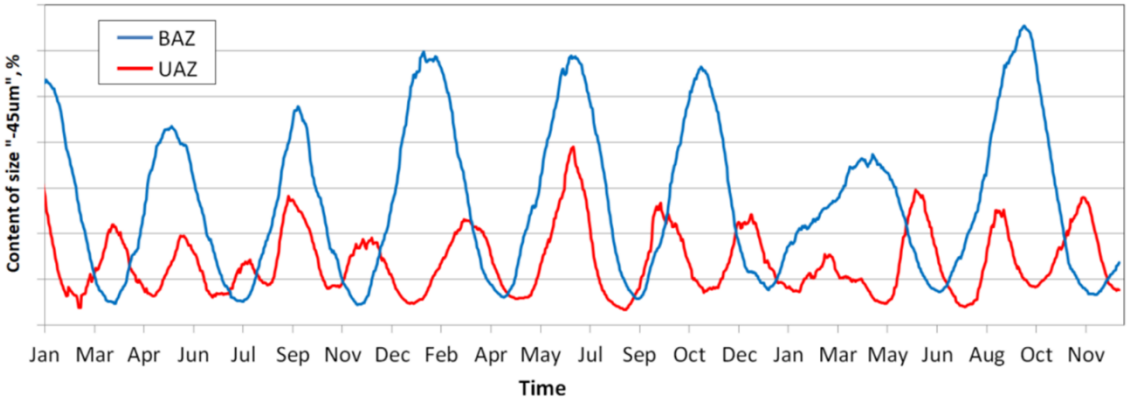

Figure 1. Fluctuations of – 45 µm seed fraction at RUSAL's Kamensk Uralsky (UAZ) and Bogoslovsk (BAZ) alumina refineries over three years.

Oscillations in the PSD may be caused by process factors such as fluctuations of the solids content in the slurry or the chemical composition of the pregnant liquor. At some refineries they are associated with operation of classifiers which accumulate large amounts of seed and function as time lag elements [6, 7]. Though the production factors are not regular, Figure 1 shows almost regular oscillations, so the reason for such oscillations should be sought in natural laws.

The classical model of population balance does not appear to apply to this system, as it indicates that fluctuations should decay under steady-state external conditions. We assumed that the stability of the oscillations is associated with an intrinsic property of the chemical system, i.e. a change in the quality of the seed surface, expressed through the relative fraction of agglomerates in the crystal population. An increase in the relative number of agglomerates promotes the adhesion process and enhances the bond between new nuclei and the seed surface. During periods of increased agglomeration, secondary nucleation reduces or stops completely. After filling energetically favorable surfaces, the particle acquires a more "rounded" shape, embryos have to fix on the flat surface where the contact is minimal. These embryos become new growth centers (a process known as birth-and-spread). New nuclei that are formed on the flat surface get cleaved by impact, and pass into suspension.

The introduction of a new property, i.e. the fraction of agglomerates, into the secondary nucleation model resulted in the following transformation of this model [8]:

$$B_0 = \left\{k_n \left(\frac{A-A_{eq}}{C}\right)^{z2} S_{sl}\right\}\left\{1 - k_s \cdot \sum_i \{S_{f.i}[1 + (\bar{\mu} - 1)f_{a.i}]\}\right\} \quad (8)$$

where:
B_0 the number of secondary nuclei passing into suspenion, 1/(m^3·s)
$f_{a,i}$ the fraction of agglomerates in the ith grade

k_s configurable constant
$S_{f.i}$ surface of particles in the *i*th grade, m^2/m^4
$\bar{\mu} = \mu_a/\mu_g$ the value expressing the ratio of two probabilities of adhesion: between the nucleus and the surface of the agglomerate and between the nucleus and the surface of the growth particle.

The probability of particle breakage also depends on the fraction of agglomerates. At a temperature of 62–67 °C (the temperature used at UAZ and BAZ refineries agglomerates do not gain sufficient strength during the agglomeration; therefore, they are more prone to degradation than separate growth particles. For this reason, we also improved the binary breakage Equation (6) by introducing the fraction of agglomerates as one of the parameters:

$$\vartheta(t,u) = k_b \gamma^p \bar{m}_1 \cdot F(u) \cdot f_a(t,u), \quad (9)$$

$$F(u) = \frac{1}{\delta\sqrt{2\pi}} exp\left(-\frac{(L_u - L^*)^2}{2\delta}\right), \quad (10)$$

where:
$F(u)$ the rate of breakage of particles of the *u*th grade, $1/(m^4 \cdot s)$
L^* the size of the most destructible particle, m
δ configurable constant.

The study of the upgraded model of the population balance showed that the model is capable of reproducing continuous oscillations in the PSD and liquor productivity with the use of a certain combination of parameters and without external influence [8].

The experience of using the upgraded population balance model shows that the model can be used to study precipitation under irregular (for the refinery) conditions and to improve control methods. It is ill-suited for solving problems of real-time control, since it requires time-consuming manual configuration and a high computational demand.

3. Deep Learning Methods

There are many deep learning methods. Recurrent neural networks (RNN) work best for describing the processes that evolve in time and depend on the previous condition of the system [9]. Figure 2 shows the RNN structure. The RNN process predicts output parameters several data points ahead by using the archive data of input and output parameters: as well as providing assumptions/plans for changing control parameters for the forecast period.

We studied several types of artificial neural networks and chose to go with the recurrent neural network with Long Short-Term Memory (LSTM) architecture [10, 11]. A deep learning network of the LSTM type consists of a sequence of cells, each of which uses signals from the input parameters and the conditions of the previous cells as input data. In addition to the standard activation function, such as the hyperbolic tangent (see Figure 3), inside the LSTM cell there is a memory mechanism (to take into account the conditions of the previous cell and to scale and/or forget them). In recent years LSTM networks have been widely used for recognition of visual images, natural languages, and texts. In our case we can also say that the RNN learns and recognizes a dynamic precipitation pattern.

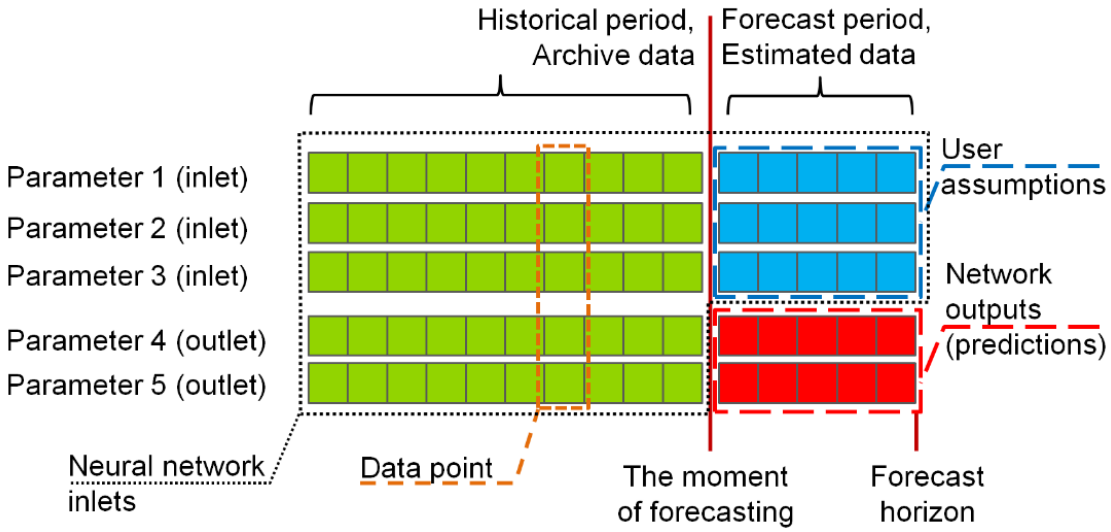

Figure 2. Structure of Recurrent Neural Network.

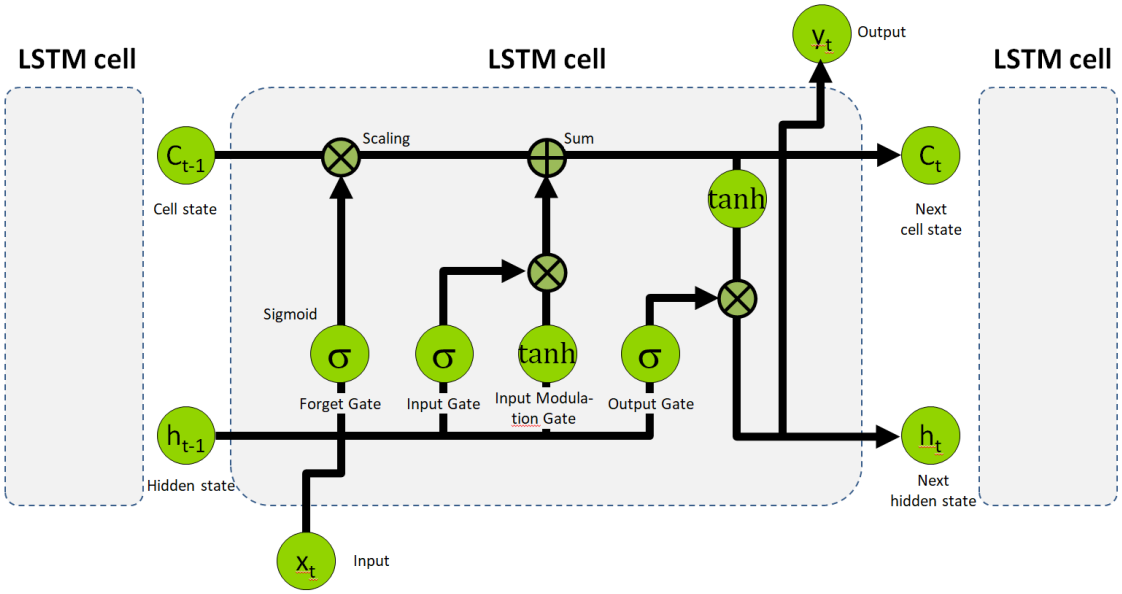

Figure 3. Structure of Long Short-Term Memory Cell.

4. Software PrecipExpert

We have combined the capabilities of the population balance method and artificial neural networks to create a new software tool for simulating the precipitation process, we have called PrecipExpert. It can be used to develop a precipitation process flow diagram, placing and connecting standard equipment (tanks, hydrocyclones, filters, etc.), or LSTM blocks can be added to it. The parameters of each element of the PFD are configured separately. The developed circuit is supplied with input information from the control system, and these inputs are improved by eliminating outliers and data gaps.

Figure 4 shows a diagram of one of the existing precipitation lines which has been developed using PrecipExpert software. In the lower part there is a graphic area displaying the results of dynamic calculations.

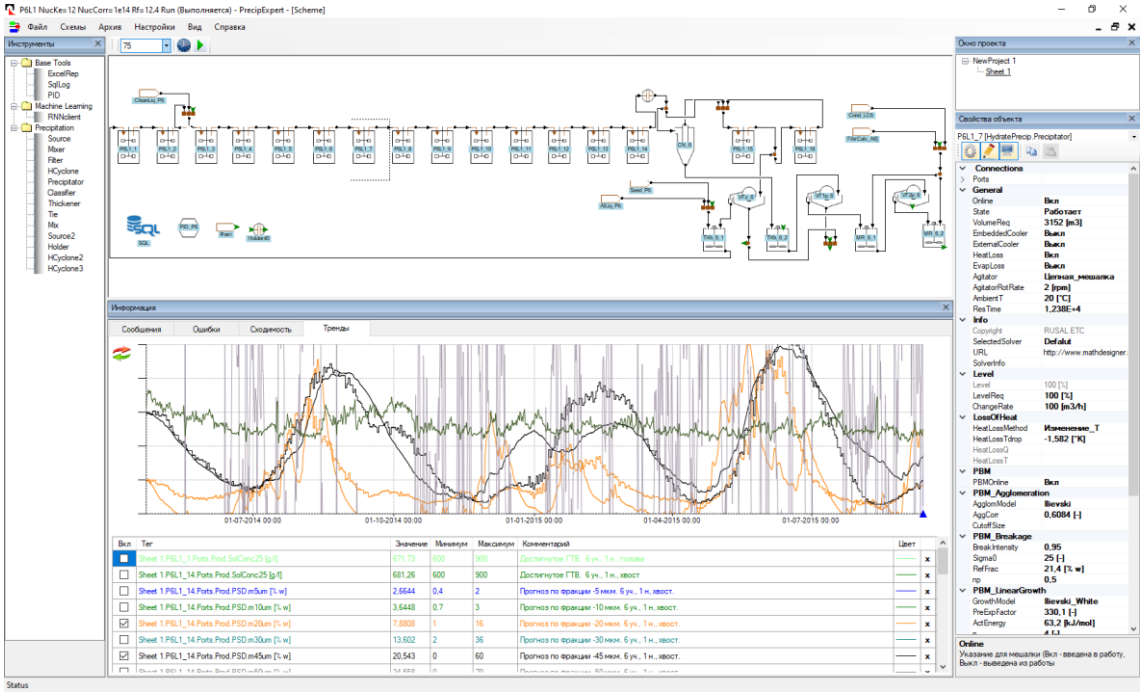

Figure 4. Population balance model made for one precipitation line in PrecipExpert.

The LSTM block representing one precipitation train consists of only one element. Figure 5 shows six blocks of this kind, each predicting a change in the crystal PSD and the liquor productivity. Combined these blocks describe the operation of the entire precipitation area at UAZ refinery. The prediction results in tabular and graphical form are presented in a separate window of the Recurrent Networks Wizard, where the operator can adjust and optimize control plans/strategy in manual mode.

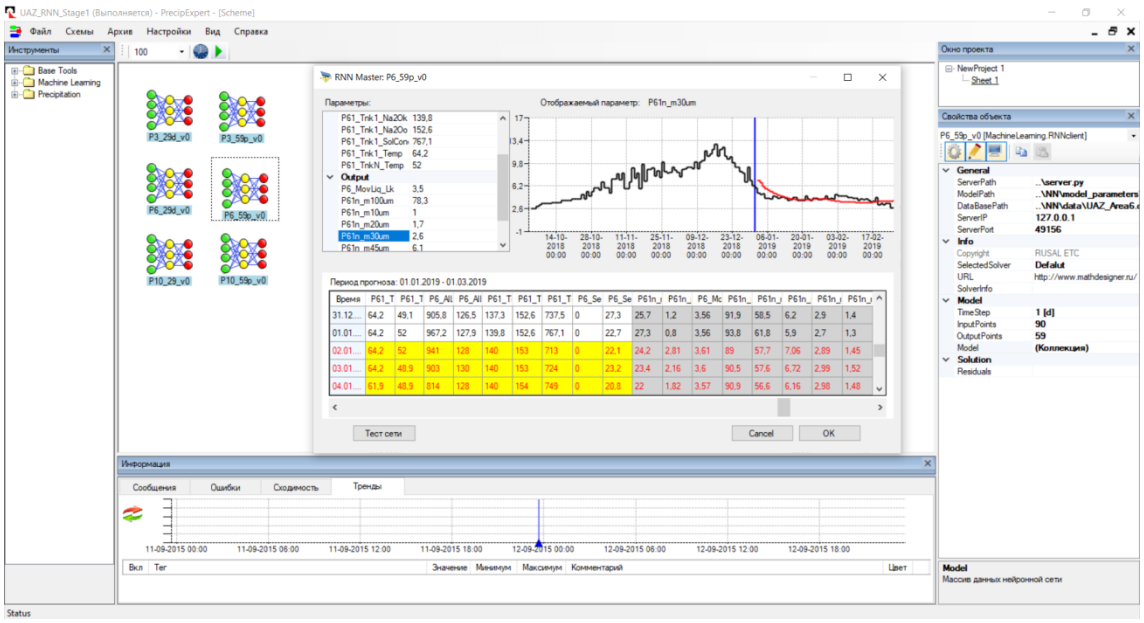

Figure 5. LSTM models for the precipitation area of UAZ refinery and user interface for working with recurrent neural networks in PrecipExpert.

5. Prediction Results

After completing several hundred trainings of artificial neural networks, the final set of network input and output parameters was generated achieving the best prediction results with a forecast horizon of 60 days (Table 2).

Table 2. List of input and output parameters of the artificial neural network.

Input parameters	Output parameters
Temperature in the head precipitator	+ 150 µm, %
Temperature in the tail precipitator	- 100 µm, %
Pregnant liquor. Feed flow	- 63 µm, %
Pregnant liquor. A	- 45 µm, %
Pregnant liquor. C	- 30 µm, %
Pregnant liquor. S	- 20 µm, %
Solids content in the head precipitator	- 10 µm, %
Seed from other areas. Volume flow	Spent liquor A/C
Seed from other areas. Content of - 45 µm	

Figure 6 shows the change in the content of - 45 µm fraction in the tail tank of the precipitation area at UAZ refinery (black line) and 60-day forecast of the LSTM model (red line). The data ranges before and after the vertical line correspond to the input and output data point ranges.

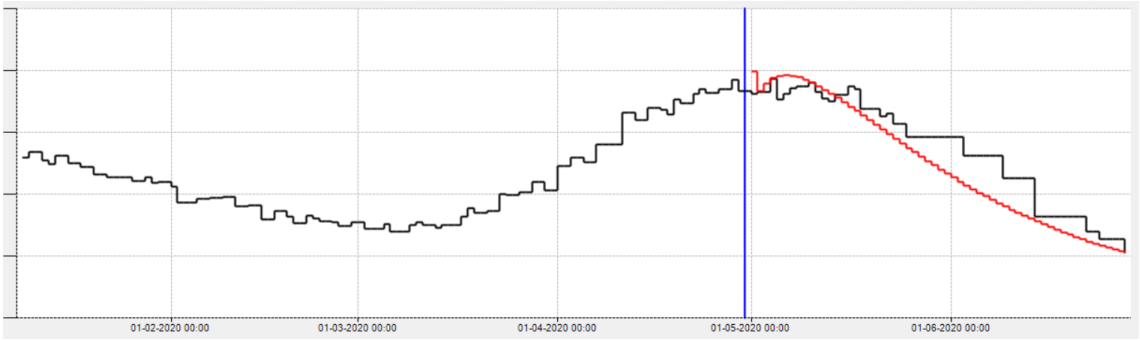

Figure 6. Historical data and 60-day prediction using the LSTM model of the – 45 µm content in the seed slurry: black line – refinery data, red line - 60-day forecast of the LSTM model.

Population balance models can provide long-term predictions of PSD changes and liquor productivity with proper tuning and the availability of appropriate input data. The Recurrent Neural Network approach also demonstrates high quality predictions but for shorter periods. The graphs in Figure 7 show a comparison of the quality of prediction made using both methods. Population balance model produced a forecast for a period of 1.5 years at a time, while recurrent neural network (having the forecast horizon equal to 60 days) required 9 refinements to cover the same time interval. Both models have approximately the same error in predicting PSD, but the PBM model calculates the molar A/C ratio of the spent liquor more accurately.

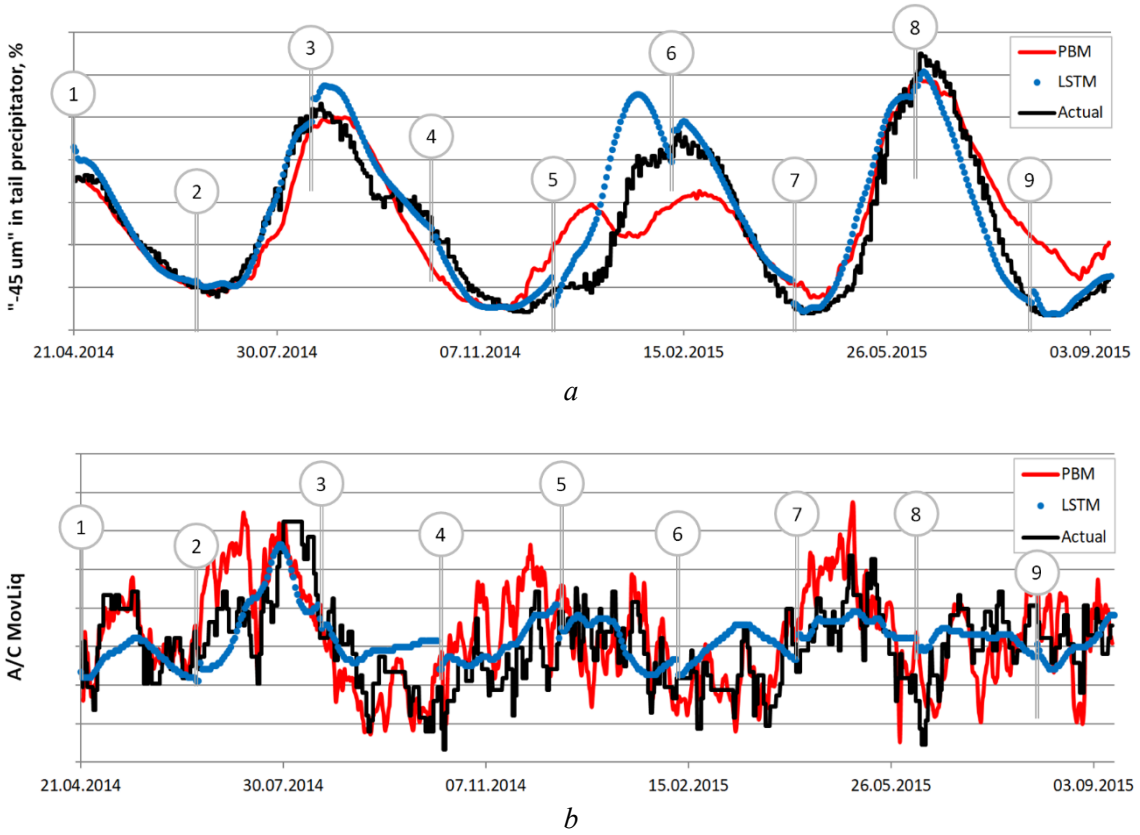

Figure 7. Comparison of the quality of forecasts made using PBM and LSTM: *a* – product – 45 µm fraction; *b* – spent liquor molar A/C ratio.

Input parameters, number of input data points, and internal characteristics (activation functions, the number of hidden layers, the method of regularization, and the loss function) of the networks were changed during the training of artificial neural networks. As a result, one network with the smallest standard error for the - 45 µm fraction was selected for each of three precipitation areas of UAZ refinery. The table shows the standard deviations of predictions for a test period of 7 years. The standard error ranges from 4.5 % to 5.3 % for - 45 µm fraction, which is considered a good result (see Table 3).

Table 3. Standard deviation of forecasts developed by LSTM.

Parameter	Area #3	Area #6	Area #10
+ 150 µm	1.39	1.37	1.30
- 100 µm	4.55	4.94	4.59
- 63 µm	6.43	6.47	6.68
- 45 µm	4.97	4.51	5.34
- 30 µm	2.32	2.47	3.54
- 20 µm	0.917	1.09	1.77
- 10 µm	0.263	0.260	0.389
Spent liquor L_k^*	0.090	0.105	0.098

* $L_k = 1.645 \bullet C_{Na2O}/C_{Al2O3} = 106/102/(A/C)$.

PrecipExpert software and precipitation models are currently being tested at the refinery. This period is required to work out the strategy for their application and to improve the personnel's confidence. The models will be tested until the end of the year. During this time, we intend to

develop and customize the optimization block, the second necessary element of the advanced control system. These results will be presented and discussed in future.

6. Conclusions

The population balance model of Bayer (gibbsite) seeded precipitation circuit has been improved for pregnant liquors with a low A/C ratio. Updated equations for secondary nucleation and particle breakage were proposed which take into account the surface quality and particle strength through the fraction of agglomerates in the population. The model accurately predicts the oscillations of particle PSD and liquor productivity in the studied industrial precipitation circuits.

Recurrent neural networks are effective for mid-term prediction of A/C ratio of the spent liquor and PSD of produced aluminum hydroxide. A set of LSTM models was trained with the use of the historical data of UAZ refinery. The obtained average correlation coefficient was > 0.93 for - 45 μm fraction in 60-days predictions.

PrecipExpert software has been developed, enabling the development of models and performance of calculations using both models.

7. References

1. Doraiswami Ramkrishna, *Population balances. Theory and Applications to Particulate Systems in Engineering*, London, Academic Press, 2000, 355 pages.
2. E.T. White, S.H. Bateman, Effect of caustic concentration on the growth rate of $Al(OH)_3$ particles, *Light Metals* 1988, 157 – 162.
3. D. Ilievski, I. Livk, An agglomeration efficiency model for gibbsite precipitation in a turbulently stirred vessel, *Chem. Eng. Science*, Vol. 61, (2006), 2010-2022.
4. I. Livk, D. Ilievski, A macroscopic agglomeration kernel model for gibbsite precipitation in turbulent and laminar flows, *Chem. Eng. Science*, Vol. 62, (2007), 3787 – 3797.
5. C. Misra, The precipitation of Bayer aluminium trihydroxide. Ph.D. thesis, University of Queensland, Australia, 1970, 236 pages.
6. J. Yin et al., Study on the oscillation phenomena of particle size distribution during the seeded agglomeration of the sodium aluminate liquors, *Light Metals* 2006, 173-176.
7. A.V. Bekker et al., Understanding oscillatory behaviour of gibbsite precipitation circuits, *Chemical engineering research and design,* 2015, 101, 113-124.
8. V.O. Golubev, T.E. Litvinova, Dynamical simulation of industrial scale gibbsite crystallization circuit, *Journal of Mining Institute*, to appear.
9. Su Yuanhang, Kuo Jay, Empirical Evaluation of Gated Recurrent Neural Networks on Sequence Modeling, *NIPS 2014 Workshop on Deep Learning*, December 2014.
10. S. Hochreiter, J. Schmidhuber, Long short-term memory, *Neural Computation*, Vol. 9 (8), 1735–1780.
11. François Chollet, *Deep Learning with Python*, NY, Manning Publications Co, 2018, 440 pages.